

All-*trans* retinoic acid is a ligand for the orphan nuclear receptor ROR β

Catherine Stehlin-Gaon^{1,4}, Dominica Willmann^{2,4}, Denis Zeyer¹, Sarah Sanglier³, Alain Van Dorsselaer³, Jean-Paul Renaud¹, Dino Moras¹ & Roland Schüle²

Retinoids regulate gene expression through binding to the nuclear retinoic acid receptors (RARs) and retinoid X receptors (RXRs). In contrast, no ligands for the retinoic acid receptor-related orphan receptors β and γ (ROR β and γ) have been identified, yet structural data and structure-function analyses indicate that ROR β is a ligand-regulated nuclear receptor. Using nondenaturing mass spectrometry and scintillation proximity assays we found that all-*trans* retinoic acid (ATRA) and several retinoids bind to the ROR β ligand-binding domain (LBD). The crystal structures of the complex with ATRA and with the synthetic analog ALRT 1550 reveal the binding modes of these ligands. ATRA and related retinoids inhibit ROR β but not ROR α transcriptional activity suggesting that high-affinity, subtype-specific ligands could be designed for the identification of ROR β target genes. Our results identify ROR β as a retinoid-regulated nuclear receptor, providing a novel pathway for retinoid action.

The orphan nuclear subfamily NR1F is composed of the retinoic acid receptor-related orphan receptors ROR α , β and γ (reviewed in ref. 1). ROR β is highly expressed in neurons of the afferent sensory pathway and in different parts of the neurophotoendocrine system. This suggests that ROR β might regulate genes that control the integration of sensory input in addition to its role in regulating the circadian clock^{2,3}. ROR β can bind as a monomer to the sequence ANNTAGGTCA, where N is any nucleotide, and activates reporter genes containing multiple copies of this motif⁴. However, no natural target gene regulated by ROR β has yet been identified. Transcriptional activation by ROR β is cell type-specific and mediated through interactions with nuclear cofactors. RORs have been shown to interact with corepressors and co-activators. The data suggest that RORs are not constitutively active but that their transcriptional potential is under regulatory control^{5,6} (reviewed in ref. 1). We previously solved the crystal structure of the rat ROR β LBD in complex with a co-activator peptide containing the second LXXLL receptor interaction motif of the co-activator SRC-1 and a fortuitous ligand stearate (STE); the ligand dependence of this nuclear receptor was confirmed using site-directed mutagenesis of key residues located in the ligand-binding pocket (LBP)⁷. Notably, the stearate molecule that was fortuitously captured from the expression host (*Escherichia coli*) seems to act as a 'filler' molecule⁸ rather than a true ligand as stearate neither activates nor antagonizes ROR β transcriptional activity. Therefore, no functional ROR β ligand had been characterized before this report. The discovery of functional ligands is an essential step toward the elucidation of the molecular pathways of a nuclear receptor action. This is an important part of the 'reverse

endocrinology' strategy to characterize the functional role of orphan receptors. RORs represent an optimal case for this approach as we could already prove the ligand dependence of ROR β action and show that the different isoforms exhibit substantial structural differences in their ligand-binding pockets, raising hopes that subtype-specific ligands could be found. The purpose of the present study was to find bona fide ligands that could be used for the identification of natural target genes regulated by ROR β and test their isotype specificity. The study is also proof of concept of a strategy using mass spectrometry as a screening tool⁸.

RESULTS

Ligand identification

In the present study, we used nondenaturing electrospray ionization mass spectrometry (ESI-MS)⁹ to identify potential ligands for ROR β . ESI-MS analysis of the ROR β LBD produced in *E. coli* showed that ROR β copurifies with stearate from the expression host⁸ (Fig. 1a). A 1:1 stoichiometry was observed but stearate binding is not quantitative as a mixture of bound and unbound species was detected. RORs are evolutionarily close to RARs although ATRA was reported not to activate RORs. Nevertheless, we wanted to check by mass spectrometry whether ATRA or related retinoids might bind to RORs. Incubation of the ROR β LBD with ATRA or the synthetic retinoid ALRT 1550 (ALRT) resulted in quantitative binding and complete replacement of stearate (Fig. 1b,c). Control experiments with other compounds demonstrated that formation of the ROR β LBD-ATRA and ROR β LBD-ALRT complexes is specific (data not shown).

¹Département de Biologie et Génétique Structurales, Institut de Génétique et de Biologie Moléculaire et Cellulaire, 1 rue Laurent Fries, 67404 Illkirch, France.

²Universitäts-Frauenklinik, Zentrum für Klinische Forschung, Klinikum der Universität Freiburg, Breisacherstrasse 66, 79106 Freiburg, Germany. ³Laboratoire de Spectrométrie de Masse Bio-Organique, Ecole de Chimie, Polymères et Matériaux, 25 rue Bequerel, 67087 Strasbourg, France. ⁴These authors contributed equally to the work. Correspondence should be addressed to D.M. (moras@igbmc.u-strasbg.fr).



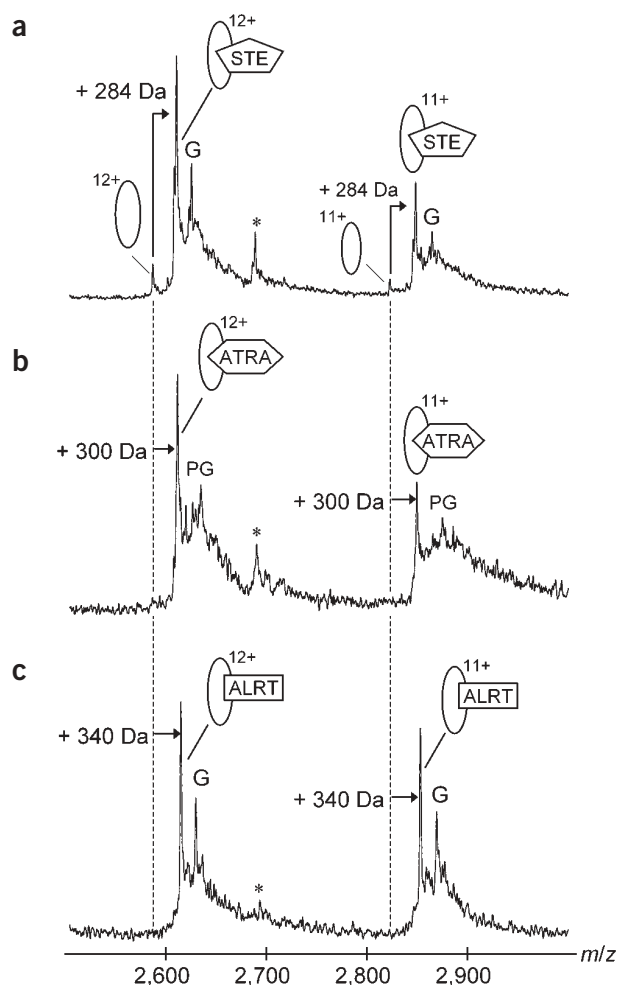


Figure 1 Nondenaturing ESI-MS analysis of ligand binding to ROR β .

(a) ROR β -stearate complex (ROR β -STE): before addition of any ligand, ~90% of the detected species correspond to the ROR β -STE complex and 10% are related to unliganded ROR β . (b) ROR β -ATRA complex: after addition of 2.5 molar equivalents of ATRA (molecular mass = 300.4 Da), the only detected species corresponds to the ROR β -ATRA complex. Neither unliganded ROR β nor the ROR β -STE complex is present in the ESI mass spectrum. (c) ROR β -ALRT 1550 complex (ROR β -ALRT): after addition of 2.5 molar equivalents of ALRT (molecular mass = 340.5 Da), the only detected species corresponds to the ROR β -ALRT complex. Neither unliganded ROR β nor the ROR β -STE complex is present in the ESI mass spectrum. The ESI-MS measured masses for the different complexes are: 31,034.5 \pm 0.5 Da for ROR β , 31,321.4 \pm 0.9 Da for ROR β -STE, 31,334.6 \pm 1.3 Da for ROR β -ATRA and 31,373.9 \pm 0.8 Da for ROR β -ALRT. Asterisk represents ROR β without the His₆-tag; G, gluconoylation of the His₆-tag; PG, phosphogluconoylation of the His₆-tag²⁸.

Waals contacts with residues of helix 5 but only two of these contacts are also observed in the ATRA and stearate complexes. As for helix 3 (H3), Ala269 is the only common residue in contact with each of the three ligands (Fig. 2c), thus confirming the correlation between the drastic effect of mutating Ala269 on ROR β function and ligand binding⁷. Other substantial differences are observed with H7, which makes a single van der Waals contact with ALRT and two additional interactions with ATRA and stearate (Fig. 2d). For ALRT, they may be compensated by two contacts with H11 and H6. In summary, the higher affinity of ATRA and ALRT (as shown in Fig. 3) can be explained by a better anchoring of their carboxylate groups, a situation that is similar to the anchoring of ATRA observed in the RAR LBD-ATRA complex, and by a larger number of van der Waals contacts. Remarkably, in all complexes (ATRA, ALRT, stearate) the ligand makes no contact with H12 (d_{\min} ~7 Å).

ATRA and ALRT 1550 are bona fide ligands for ROR β

To verify ATRA as a bona fide ligand of ROR β , we tested specific binding of [³H]ATRA to the *E. coli*-expressed ROR β LBD in scintillation proximity assays (Fig. 3a). Our analysis demonstrates that [³H]ATRA binds in a specific manner to the ROR β LBD. The control (mock extract) showed only nonspecific binding of the radioligand. Competition binding assays revealed a K_d of 280 nM for ATRA, thus demonstrating specific ligand binding *in vitro* (Fig. 3b). We next asked whether unlabeled retinoids compete for binding of [³H]ATRA to the ROR β LBD. ATRA, ALRT, and all-*trans*-4-oxo-RA (AT4ORA) bound to the ROR β LBD with a half-maximal inhibitory concentration (IC_{50}) in the nanomolar range. Competition by ALRT (K_i = 1.6 \times 10⁻⁷ M) or ATRA (K_i = 2.8 \times 10⁻⁷ M) is better than that by AT4ORA (K_i = 8 \times 10⁻⁷ M). Notably, we observed no substantial competition by the RAR antagonist RO 41-5253, by stearate, or by the putative ROR α ligand cholesterol¹¹. Indeed, the affinity of these compounds is too low to calculate their K_i values (Fig. 3b). The control estradiol did not compete at all, further confirming specific binding of these retinoids. To determine whether retinoids modulate ROR β activity *in vivo*, we assayed ATRA and selected retinoids in transient transfection experiments with Gal-ROR β LBD expression constructs and Gal-dependent reporters in HT22 cells (Fig. 3c). The functional assays show that the retinoid ligands strongly antagonized transactivation by ROR β . ALRT is the most potent antagonist with an IC_{50} value of 3.9 \times 10⁻¹¹ M, followed by ATRA (IC_{50} = 1.5 \times 10⁻¹⁰ M) and AT4ORA (IC_{50} = 5.2 \times 10⁻¹⁰ M). Both the putative ROR α ligand cholesterol¹¹ and the pseudo ligand stearate failed to influence ROR β transcriptional activity. Estradiol served as a control and did not inhibit ROR β activity. Reporter activity is not influenced by any retinoid in the absence of Gal-ROR β LBD

Crystal structures of ATRA and ALRT complexes

We then crystallized the ROR β LBD-ATRA and ROR β LBD-ALRT complexes in the presence of a peptide containing the second nuclear receptor-interacting domain of the co-activator SRC-1 under the previously reported conditions⁷. The overall conformation of the LBD in both complexes is similar (r.m.s. deviation of 0.46 Å for all atoms) (Fig. 2a). The size of the LBP, an indicator of the protein flexibility, fluctuates from 753 Å³ in the ROR β LBD-ATRA structure to 820 Å³ in the ROR β LBD-ALRT. The ligands occupy 38% and 39% of the cavity, respectively. In line with the higher affinity of the retinoid ligands, their electron density is well defined (Fig. 2b). Compared with the carboxylate group of stearate, the carboxylate groups of both retinoids are positioned closer to the two conserved arginine residues Arg306 and Arg309 (Fig. 2c,d). However, in contrast to the situation in RAR¹⁰, the carboxylate groups of ATRA and ALRT still make only water-mediated hydrogen bonds with the arginines (Fig. 2c). The other bond observed in the ROR β LBD-STE complex, a hydrogen bond between the carboxylate group of stearate and the side chain amino group of Gln265, is replaced by two hydrogen bonds between the carboxylate group of the retinoid ligands and the main chain NH atoms of Glu228 and Tyr229. As in the stearate-bound complex, the hydrophobic tail of ATRA and ALRT is in contact with several LBP residues, which vary from one complex to another. For example, ALRT makes six van der

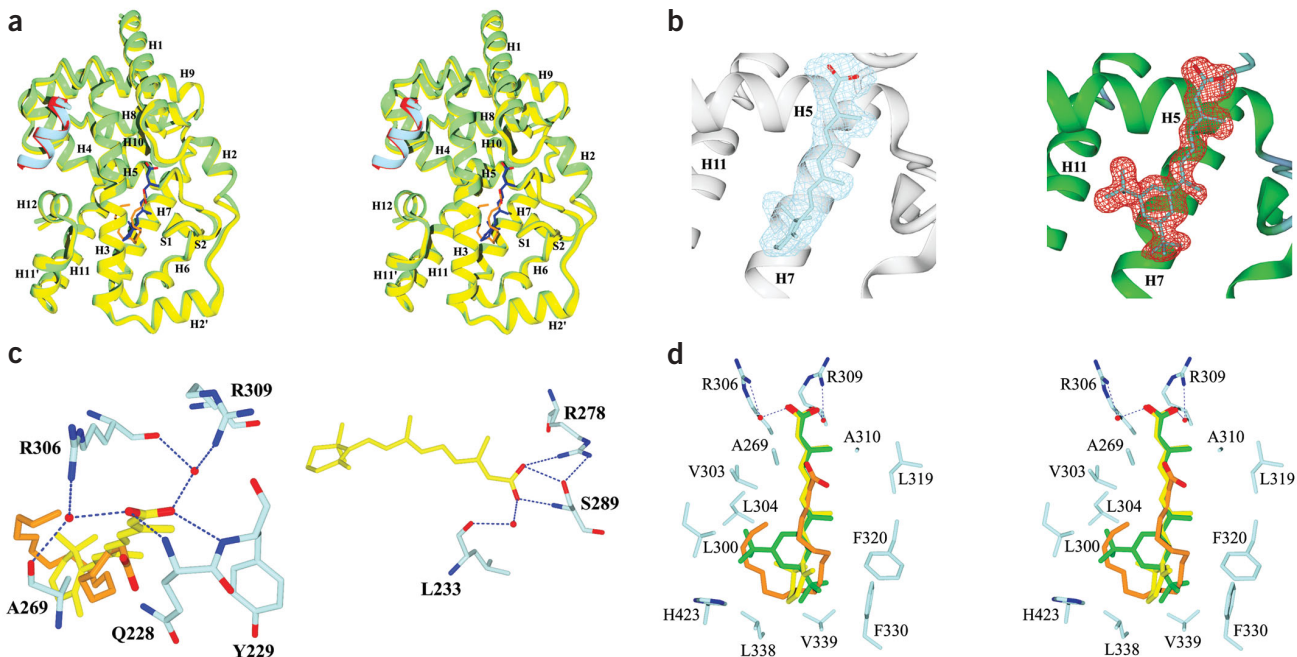


Figure 2 Crystal structures of the ROR β LBD in complex with ATRA and ALRT. (a) Stereo view of the backbone superposition of the structures of the ROR β LBD (yellow) in complex with stearate (orange) and the SRC-1 peptide (red) (PDB entry 1K4W) and of the ROR β LBD (green) in complex with ATRA (dark blue) and the SRC-1 peptide. (b) Electron density omit maps of the bound ligands. The maps were calculated at 2.1 Å for ATRA (left) and 1.5 Å for ALRT (right). Contour levels are 2.0 σ and 2.5 σ , respectively; labels refer to the canonical helix numbering. (c) Anchoring of the carboxylate of ATRA in two different LBDs. Left, ATRA (yellow) and stearate (orange) in ROR β ; the superposition was made on the protein atoms. Right, ATRA in hRAR γ (PDB entry 2LBD). In ROR β , ATRA forms two water mediated hydrogen bonds to Arg306 and Arg309 whereas in RAR it forms one direct hydrogen bond to Arg278. (d) Stereo view of the superposition of stearate (orange), ATRA (yellow) and ALRT (green) in the ROR β ligand-binding pocket. The protein atoms follow the standard color code.

expression constructs (data not shown). We note that the amount of retinoids required to displace 50% of [3 H]ATRA binding is much higher than the amount required for 50% receptor inhibition. A similar observation was reported for the binding and the transcriptional response of RAR to 4-oxo-retinoids¹². The reason for this behavior is unknown at present. Notably, however, ATRA inhibits ROR β activity even in the presence of a 100-fold molar excess of the RAR antagonist RO 41-5253, which neither binds to the receptor (Fig. 3b) nor influences ROR β activity (Fig. 3d). Compared with GAL4 alone, GAL4-RAR behaves as a strong transcriptional repressor in the absence of ligand and as a strong transcriptional activator in presence of ATRA (Fig. 3d, lanes 1–4). In the presence of ATRA, addition of RO 41-5253 reduces GAL4-RAR transcriptional activity back to the GAL4 basal level, thus demonstrating that the RAR antagonist blocks the agonist action of ATRA on RAR (Fig. 3d, compare lanes 1, 4 and 8). These data convincingly demonstrate that the effect of ATRA is mediated by ROR β but not by RARs whose transactivation activity is blocked by RO 41-5253 (Fig. 3). Similar results were obtained with ALRT (data not shown). The efficacy of the tested retinoids in transactivation assays is well within the concentration range of retinoids in cells¹³, thus demonstrating that retinoids are physiological ligands *in vivo*.

Isotype specificity

To further validate the specificity of these ligands we tested whether the retinoids could modulate ROR α activity (Fig. 3f). Notably, none of these ROR β -specific ligands inhibited ROR α transcriptional activity, nor did the control estradiol or the pseudo ligand stearate. On the

other hand, both ATRA and ALRT also inhibited ROR γ activity (data not shown). As ROR β exhibits a tissue-specific expression pattern, we analyzed the effect of ATRA on ROR β activity in different cell lines. ATRA antagonized transactivation by ROR β in the neuronal cell lines HT22 and Neuro2A (Fig. 3g). In contrast, ATRA showed no effect in cells such as NIH3T3, 293 or P19. This indicates that regulation of ROR β activity by ATRA is dependent on cell type. In summary, our data demonstrate that ATRA and ALRT selectively bind to and modulate the transcriptional activity of ROR β . We identify ATRA as a physiological, bona fide ROR β ligand.

DISCUSSION

We demonstrated that ATRA is a bona fide, physiological ligand for ROR β . ATRA binds ROR β *in vitro* and controls receptor activity *in vivo*. In contrast, the fortuitous 'filler' molecule stearate neither competes for binding of ATRA to ROR β nor affects ROR β transcriptional activity. Our data support the existence of a novel retinoid signaling cascade directly regulated by ROR β , in addition to the well characterized RAR- and RXR-mediated pathways. Nature could have exploited the dual affinity of ATRA for ROR β and RARs to set up a crosstalk between these pathways. The inhibition of ROR β by ATRA could counteract the activation of RARs by downregulating RAR target genes as part of a regulatory control mechanism. Nevertheless, it remains to be demonstrated whether ATRA is the only natural ROR β ligand. Because retinoids such as ATRA and ALRT regulate ROR β function, our data support the idea that the previously described constitutive transcriptional activity of this orphan nuclear receptor is con-

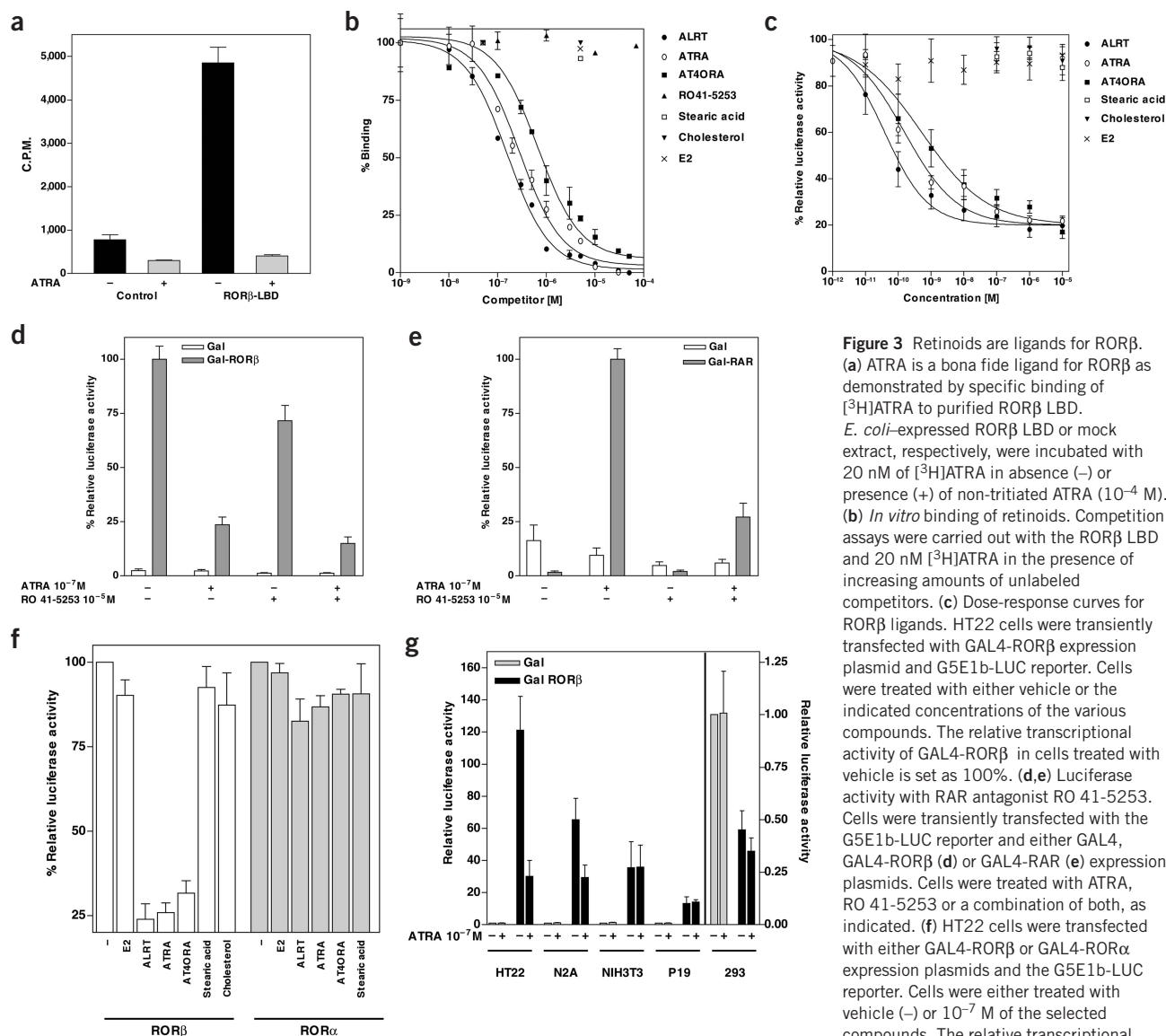


Figure 3 Retinoids are ligands for ROR β .

(a) ATRA is a bona fide ligand for ROR β as demonstrated by specific binding of [³H]ATRA to purified ROR β LBD.

E. coli-expressed ROR β LBD or mock extract, respectively, were incubated with 20 nM of [³H]ATRA in absence (-) or presence (+) of non-tritiated ATRA (10⁻⁴ M).

(b) *In vitro* binding of retinoids. Competition assays were carried out with the ROR β LBD and 20 nM [³H]ATRA in the presence of increasing amounts of unlabeled competitors.

(c) Dose-response curves for ROR β ligands. HT22 cells were transiently transfected with GAL4-ROR β expression plasmid and G5E1b-LUC reporter. Cells were treated with either vehicle or the indicated concentrations of the various compounds. The relative transcriptional activity of GAL4-ROR β in cells treated with vehicle is set as 100%.

(d,e) Luciferase activity with RAR antagonist RO 41-5253. Cells were transiently transfected with the G5E1b-LUC reporter and either GAL4, GAL4-ROR β (d) or GAL4-RAR (e) expression plasmids. Cells were treated with ATRA, RO 41-5253 or a combination of both, as indicated.

(f) HT22 cells were transfected with either GAL4-ROR β or GAL4-ROR α expression plasmids and the G5E1b-LUC reporter. Cells were either treated with vehicle (-) or 10⁻⁷ M of the selected compounds. The relative transcriptional activity of either GAL4-ROR β or GAL4-

ROR α in cells treated with vehicle is set as 100%. (g) ATRA-regulated activity of ROR β in different cell lines. Cells were transiently transfected with the G5E1b-LUC reporter and either GAL4 or GAL4-ROR β expression plasmids. Cells were treated with either vehicle (-) or ATRA. Relative transcriptional activity of GAL4 in cells treated with vehicle is set as 1.

ROR α in cells treated with vehicle is set as 100%. (g) ATRA-regulated activity of ROR β in different cell lines. Cells were transiently transfected with the G5E1b-LUC reporter and either GAL4 or GAL4-ROR β expression plasmids. Cells were treated with either vehicle (-) or ATRA. Relative transcriptional activity of GAL4 in cells treated with vehicle is set as 1.

trolled by antagonistic ligands. Notably, a similar mechanism has been described for the regulation of the orphan nuclear receptors CAR β by androstane metabolites¹⁴ and ERR3 by diethylstilbestrol and tamoxifen¹⁵⁻¹⁷. The apparent discrepancy between the transcriptional effect of ATRA and ALRT and the agonist-like conformation observed in the corresponding ROR β LBD complex crystal structures can be explained by the partial antagonist character of ATRA and the other tested retinoids observed *in vivo* (only ~70% repression of ROR β activity in transactivation assays). The conformation of a nuclear receptor LBD in complex with a partial agonist or partial antagonist is not dictated by the ligand only. An LBD bound to such a ligand is not firmly locked in a unique conformation but is in dynamic equilibrium, and the presence of a cofactor can shift this equilibrium. Conversely, in the case of the ER β LBD-genistein complex, an antagonist-like con-

formation is observed in absence of co-activator peptide¹⁸. The crystal packing may also have a role in the selection of a given conformation as is the case for the apo PPAR γ LBD dimer¹⁹, the apo PXR LBD²⁰ and the RXR-RAR LBD heterodimer²¹. In the case of ROR β , the lack of interaction between H12 and the various ligands provides a good rationale for the partial antagonist character of the ligands, linked to a looser anchoring of H12. The presence of ATRA and ALRT would then allow for an equilibrium between several possible conformations, but the presence of the co-activator peptide shifts the equilibrium toward the agonist-like structure. This correlates with the low affinity of ATRA for ROR β *in vitro* ($K_d = 280$ nM) and emphasizes its partial antagonist character *in vivo* (only ~70% repression of ROR β activity in transactivation assays). Our data show that ROR β activity is antagonized by ATRA in neuronal cells (HT22) but not in cells such as

Table 1 Data collection and refinement statistics

Ligand complex	ATRA	ALRT
Source	ESRF BM14	SLS X06SA
Wavelength (Å)	0.976205	1.0100
Unique reflections	19,344	53,123
Resolution range ^a (Å)	20.0–2.10 (2.17–2.10)	20.0–1.50 (1.55–1.50)
Completeness (%)	100.0	100.0
Multiplicity	6.6	8.8
$\langle I / \sigma \rangle^a$	22 (8)	32 (13)
$R_{\text{sym}}^{\text{a,b}}$ (%)	4.5 (17.5)	6.1 (16.7)
Reflections used in refinement	19,024	52,613
Resolution range (Å)	20.0–2.10	20.0–1.50
$R_{\text{cryst}}^{\text{c}}$ (%)	20.8	20.1
$R_{\text{free}}^{\text{d}}$ (%)	23.3	22.0
Water molecules	129	381
R.m.s. deviations		
Bond lengths (Å)	0.007	0.006
Bond angles (°)	1.120	1.077
Average B -values (Å ²)		
All non-hydrogen atoms	34.5	25.4
Protein + peptide	34.0	22.8
Ligand	44.4	38.4
Water molecules	41.2	38.7

^aValues in parentheses are for the highest-resolution shell. ^b $R_{\text{sym}}(I) = \sum_{hkli} |I_{hkli} - \langle I_{hkli} \rangle| / \sum_{hkli} I_{hkli}$, where $\langle I_{hkli} \rangle$ is the average intensity of the multiple I_{hkli} observations for symmetry-related reflections. ^c $R_{\text{cryst}} = \sum_{hkli} |F_o - F_c| / \sum_{hkli} |F_o|$. ^d $R_{\text{free}} = \sum_{hkli \in T} |F_o - F_c| / \sum_{hkli \in T} |F_o|$, where the T set (5% of reflections) is omitted in the refinement.

NIH3T3, 293 or P19. Thus, the ability of ATRA to control ROR β activity is cell-type dependent. A neuronal-specific co-repressor selective for ROR α , hairless, has been described⁶. Therefore, it is not unreasonable to hypothesize that similar ROR β -specific repressors exist that control retinoid signaling by ROR β in a cell type-specific manner. Notably, retinoid signaling by RAR or RXR inhibits CLOCK–BMAL-1-mediated transcriptional activation of circadian clock genes in the peripheral vasculature²². As ROR β participates in the regulation of the circadian clock, our data might suggest a possible link between retinoid signaling by ROR β and the regulation of the central circadian rhythm.

Finally, we demonstrate that ATRA and ALRT inhibit ROR β but not ROR α transcriptional activity. Conversely, cholesterol, a putative ROR α ligand, neither bound to nor modulated ROR β activity. Furthermore, we found a similar inhibitory effect of ATRA and ALRT on ROR γ activity (data not shown). This suggests the possibility of designing subtype-specific synthetic ligands (at least α versus β or γ). Indeed, a docking study based on the homology model predicted that ATRA should not modulate ROR α activity; this is functionally confirmed (Fig. 3d,e). Moreover, the structure-based prediction is that hydrophobic molecules with a carboxylic head are good ROR β ligand candidates. The analysis of the pocket indicates anchoring points for the design of subtype-specific ROR ligands. One could for instance combine the ‘primary’ (arginines as for ATRA and ALRT) and ‘secondary’ (glutamines as for stearate) anchoring sites to get higher affinity ROR β ligands. After this paper was submitted, the structure of the ROR α LBD was published¹¹, revealing cholesterol as a fortuitous ligand that was able to activate ROR α . We tested the subtype specificity and found that cholesterol, similarly to stearate, neither competes for binding of ATRA to ROR β nor affects ROR β transcriptional activity.

In summary, the identification of ATRA as a bona fide ligand for ROR β initiates not only the development of potent and selective ROR subtype-specific ligands but also the identification of ligand-dependent ROR target genes. This will facilitate the understanding of the molecular pathways of ROR action.

METHODS

Electrospray mass spectrometry. Before mass analysis, the ROR β LBD purification buffer was exchanged against 100 mM ammonium acetate with a gel filtration column (NAP-5, Amersham Pharmacia) and concentrated on a microconcentrator (Centricon, Millipore). Experiments involving ligands were done by adding 2.5 molar equivalents of ligand to 2.4 nmol of ROR β , followed by 15 min incubation at 4 °C. We used a 2.5-fold molar excess of ligand as a standard in our mass spectrometry experiments for two reasons: (i) to be able to detect ligands even with poor affinities (50–100 μM) as we were first screening for a ligand to stabilize the LBD for crystallization, and (ii) to assess the specificity of the binding: with a 2.5-fold molar excess, nonspecific binding would also lead to the appearance of bis-adducts, which could not be seen with only a 1:1 ratio. Before ESI-MS analysis, samples were diluted to a final concentration of 15 μM in 50 mM ammonium acetate (pH 6.8) and were continuously infused into the ESI ion source of an ESI-TOF instrument (LCT, Micromass) at a flow rate of 6 $\mu\text{l min}^{-1}$. To prevent dissociation in the gas phase during the ionization and desorption process, the cone voltage was optimized to 5–10 V. Mass data were acquired in the positive ion mode on a mass range of 1,000–5,000 m/z . Calibration of the instrument was carried out by using multiply charged ions produced by horse heart myoglobin diluted to 2 μM in a 1:1 water/acetonitrile mixture (v/v) acidified with 1% (v/v) formic acid. The characterization of stearate as a ‘filler’ molecule has been described⁸.

Structure determination. The ROR β LBD was co-crystallized with a three-fold molar excess of either ATRA or ALRT and a three-fold molar excess of the SRC-1 peptide (residues 686–700) under similar conditions as described for the ROR β LBD–STE–SRC-1 peptide complex⁷. Crystals, measuring up to 300 \times 160 \times 100 μm , grew within two weeks at 22 °C. The crystals were cryoprotected with a film of viscous paraffin oil and then flash frozen in liquid ethane at liquid nitrogen temperature. X-ray diffraction data were collected from a single frozen crystal at the BM14-CRG beamline at the European Synchrotron Radiation Facility (ESRF; Grenoble, France) for ATRA and the Swiss Light Source (SLS) X06SA (Zurich, Switzerland) for ALRT, and processed using DENZO and SCALEPACK²³ (Table 1). The crystals were isomorphous (space group $P2_12_12_1$) with unit cell parameters $a = 52.20$ Å, $b = 58.13$ Å, $c = 106.14$ Å for the ROR β LBD–ATRA complex and $a = 52.82$ Å, $b = 58.34$ Å, $c = 105.67$ Å for the ROR β LBD–ALRT complex. The average B -factor of the diffraction data (Wilson plot) is 32 Å² and 23 Å² for ATRA and ALRT complexes, respectively. The structure of both complexes was solved by molecular replacement with AMoRe²⁴ using the ROR β LBD–STE complex as a starting model, and refined using CNS²⁵. ATRA and ALRT were built using Quanta (MSI). The final refined models comprise 244 residues from the ROR β LBD, 10 residues from the peptide, one ligand, and 129 or 381 water molecules. The probe-occupied volume of the cavity was calculated with VOIDOO²⁶ using a probe radius of 1.4 Å.

Cell culture and transient transfection experiments. HT22 cells were cultured in DMEM supplemented with 5% (v/v) delipidated FCS, penicillin, streptomycin and glutamine. Experiments in presence of cholesterol were done as described¹¹. The G5E1b-LUC reporter plasmid, pCMX-Gal, pCMX-Gal-RAR α , pCMX-Gal-ROR α , and pCMX-Gal-ROR β (201–459) expression plasmids are described⁴. Transient transfection assays were carried out in 24-well plates (0.5×10^5 cells per well) with DOTAP lipofection (Roche Molecular Biochemicals) according to the manufacturer’s protocol. Luciferase activity was assayed as recommended by the manufacturer (Promega) in a microplate luminometer (EG & G Berthold). Relative light units were normalized according to ref. 27. All experiments were repeated at least five times.

Ligand-binding assays. Scintillation proximity assays were done with purified, bacterially expressed His₆-tagged ROR β -LBD⁷. Ni-NTA flash plates (96-well, NEN) were incubated with saturating amounts of protein (capacity of plates

5–10 pmol/well). Binding was carried out for 1 h at 4 °C. After washing with binding buffer (50 mM Tris, pH 7.6, 150 mM NaCl, 0.2% (v/v) NP-40, 0.1% (v/v) Triton X-100) all-*trans*-[20-methyl-³H]retinoic acid (60 Ci mmol⁻¹, NEN) was diluted in binding buffer (100 µl) to a final concentration of 20 nM. Unlabeled competing ligands were serially diluted in binding buffer and added to final concentrations ranging from 1 nM to 0.1 mM. Plates were shaken at 25 °C for 2 h. Radioactivity was measured for 1 min per well with a Packard Topcount. All concentrations were assayed in triplicate and the results were averaged. Values from wells devoid of competitor represented 100% binding. To determine the K_d , nonlinear regression analysis of the competition curves was carried out using Prism 3 (GraphPad).

Coordinates. The atomic coordinates of the ROR β -ATRA-SRC-1 peptide and ROR β -ALRT-SRC-1 peptide complexes have been deposited in the PDB (accession codes 1N4H and 1NQ7, respectively).

ACKNOWLEDGMENTS

We thank M. Salvati from Bristol-Myers Squibb for the gift of ALRT 1550 and M. Klaus from Roche for the gift of RO 41-5253 and all-*trans*-4-oxo retinoic acid, P. Eberling for peptide synthesis, B. Blumberg for advice in performing scintillation proximity assays, P. Carpentier for support on ESRF beamline BM14 CRG and C. Schulze-Briese for support on the SLS X065A beamline, J. Cavarelli for help with the ALRT-complex data, and G. Tocchini-Valentini, V. Lamour and P. Hublitz for useful discussions. This work was supported by grants from the Deutsche Forschungsgemeinschaft to R.S. and by funds from the Centre National de la Recherche Scientifique, the Institut National de la Santé et de la Recherche Médicale, Université Louis Pasteur de Strasbourg and the Fond National de la Science to the Strasbourg Génopole. We acknowledge the financial support of the European Union for the international research project SPINE. S.S. acknowledges a grant from the CNRS and Eli Lilly.

COMPETING INTERESTS STATEMENT

The authors declare that they have no competing financial interests.

Received 28 October 2002; accepted 31 July 2003

Published online at <http://www.nature.com/naturestructuralbiology/>

1. Jetten, A., Kurebayashi, S. & Ueda, E. The ROR nuclear orphan receptor subfamily: critical regulators of multiple biological processes. *Prog. Nucl. Acid Res. Mol. Biol.* **69**, 205–247 (2001).
2. Preitner, N. *et al.* The orphan nuclear receptor REV-ERB α controls circadian transcription within the positive limb of the mammalian circadian oscillator. *Cell* **110**, 251–260 (2002).
3. Ueda, H.R. *et al.* A transcription factor response element for gene expression during circadian night. *Nature* **418**, 534–539 (2002).
4. Greiner, E.F. *et al.* Functional analysis of retinoid Z receptor β , a brain-specific nuclear orphan receptor. *Proc. Natl. Acad. Sci. USA* **93**, 10105–10110 (1996).
5. Greiner, E.F. *et al.* Differential ligand-dependent protein-protein interactions between nuclear receptors and a neuronal-specific cofactor. *Proc. Natl. Acad. Sci. USA* **97**, 7160–7165 (2000).
6. Moraitis, A.N., Giguère, V. & Thompson, C.C. Novel mechanism of nuclear receptor corepressor interaction dictated by activation function 2 helix determinants. *Mol. Cell. Biol.* **22**, 6831–6841 (2002).
7. Stehlin, C. *et al.* X-ray structure of the orphan nuclear receptor ROR β ligand-binding domain in the active conformation. *EMBO J.* **20**, 5822–5831 (2001).
8. Potier, N. *et al.* Using non-denaturing mass spectrometry to detect fortuitous ligands in orphan receptors. *Protein Sci.* **12**, 725–733 (2003).
9. Loo, J.A. Electrospray ionization mass spectrometry: a technology for studying noncovalent macromolecular complexes. *Int. J. Mass Spectrom.* **200**, 175–186 (2000).
10. Renaud, J.P. *et al.* Crystal structure of the RAR- γ ligand-binding domain bound to all-*trans* retinoic acid. *Nature* **378**, 681–689 (1995).
11. Kallen, J.A. *et al.* X-ray structure of the hROR α LBD at 1.63 Å. Structural and functional data that cholesterol or a cholesterol derivative is the natural ligand of ROR α . *Structure* **10**, 1697–1707 (2002).
12. Blumberg, B. *et al.* Novel retinoic acid receptor ligand in *Xenopus* embryos. *Proc. Natl. Acad. Sci. USA* **93**, 4873–4878 (1996).
13. Kurlandsky, S.B. *et al.* Plasma delivery of retinoic acid to tissues in the rat. *J. Biol. Chem.* **270**, 17850–17857 (1995).
14. Forman, B.M. *et al.* Androstane metabolites bind to and deactivate the nuclear receptor CAR- β . *Nature* **395**, 612–615 (1998).
15. Tremblay, G.B. *et al.* Diethylstilbestrol regulates trophoblast stem cell differentiation as a ligand of orphan nuclear receptor ERR β . *Genes Dev.* **15**, 833–838 (2001).
16. Coward, P., Lee, D., Hull, M.V. & Lehmann, J. 4-Hydroxytamoxifen binds to and deactivates the estrogen-related receptor γ . *Proc. Natl. Acad. Sci. USA* **98**, 8880–8884 (2001).
17. Greschik, H. *et al.* Structural and functional evidence for ligand-independent transcriptional activation by the estrogen-related receptor 3. *Mol. Cell* **9**, 303–313 (2002).
18. Pike, A.C.W. *et al.* Structure of the ligand-binding domain of oestrogen receptor β in the presence of a partial agonist and a full antagonist. *EMBO J.* **18**, 4608–4618 (1999).
19. Nolte, R.T. *et al.* Ligand binding and co-activator assembly of the peroxisome proliferator-activated receptor- γ . *Nature* **395**, 137–143 (1998).
20. Watkins, R.E. *et al.* The human nuclear xenobiotic receptor PXR: structural determinants of directed promiscuity. *Science* **292**, 2329–2333 (2001).
21. Bourguet, W. *et al.* Crystal structure of a heterodimeric complex of RAR and RXR ligand-binding domains. *Mol. Cell* **5**, 289–298 (2000).
22. McNamara *et al.* Regulation of CLOCK and MOP4 by nuclear hormone receptors in the vasculature: a humoral mechanism to reset a peripheral clock. *Cell* **105**, 877–889 (2001).
23. Otwinowski, Z. & Minor, W. Processing of X-ray diffraction data collected in oscillation mode. *Methods Enzymol.* **276**, 307–326 (1997).
24. Navaza, J. AMoRe: an automated package for molecular replacement. *Acta Crystallogr. A* **50**, 157–163 (1994).
25. Brünger, A.T. *et al.* Crystallography & NMR system: a new software suite for macromolecular structure determination. *Acta Crystallogr. A* **47**, 110–119 (1998).
26. Kleywegt, G.J. & Jones, T.A. Detection, delineation, measurement and display of cavities in macromolecular structures. *Acta Crystallogr. D* **50**, 178–185 (1994).
27. Müller, J.M. *et al.* The transcriptional coactivator FHL2 transmits Rho signals from the cell membrane into the nucleus. *EMBO J.* **21**, 736–748 (2002).
28. Geoghegan, K.F. *et al.* Spontaneous α -N-6-phosphogluconoylation of a 'His tag' in *Escherichia coli*: the cause of extra mass of 258 or 178 Da in fusion proteins. *Anal. Biochem.* **267**, 169–184 (1999).